

Biotic-Abiotic Interface Between the Body and the Artificial Limb

Abstract

Intraosseous transcutaneous amputation prostheses (ITAPs) may be able to overcome the problems that stem from the nonuniform distribution of pressure seen in the conventional stump-socket prosthetic replacement devices. While transcutaneous devices have had limited success in amputees. By optimizing the attachment of the skin to the prosthetic, ITAPs may become clinically viable options. Our team has developed a modified titanium construct with a specially machined surface to increase the adherence of tissue as well as scaffold. A Computer Aided Biology (CAB) Tool was utilized to fabricate polycaprolactone (PCL) scaffolds with a specific three-dimensional architecture. The fabricated PCL scaffold had a tensile strength similar to skin, and when it was printed on titanium constructs, the presence of the machined surface greatly increased the its adhesion to the titanium. The antibacterial properties of titanium dioxide anatase, silver nanoparticles, and chlorhexidine diacetate mixed in either type I collagen or hyaluronic acid (HA). The addition of 1% w/w chlorhexidine diacetate in HA resulted in a 71% decrease in bacteria seen in non-treated HA. When the machined titanium constructs were implanted into a subcutaneous rat model, the tensile strength of the titanium-skin interface was significantly higher in machined constructs as compared with polished or acid etched constructs. These results show promise in developing a novel engineered titanium construct that promotes effective adhesion between the titanium-skin interface.

REPORT DOCUMENTATION PAGE				<i>Form Approved OMB No. 0704-0188</i>	
<small>The public reporting burden for this collection of information is estimated to average 1 hour per response, including the time for reviewing instructions, searching existing data sources, gathering and maintaining the data needed, and completing and reviewing the collection of information. Send comments regarding this burden estimate or any other aspect of this collection of information, including suggestions for reducing the burden, to the Department of Defense, Executive Services and Communications Directorate (0704-0188). Respondents should be aware that notwithstanding any other provision of law, no person shall be subject to any penalty for failing to comply with a collection of information if it does not display a currently valid OMB control number.</small>					
PLEASE DO NOT RETURN YOUR FORM TO THE ABOVE ORGANIZATION.					
1. REPORT DATE (DD-MM-YYYY)		2. REPORT TYPE		3. DATES COVERED (From - To)	
4. TITLE AND SUBTITLE				5a. CONTRACT NUMBER	
				5b. GRANT NUMBER	
				5c. PROGRAM ELEMENT NUMBER	
6. AUTHOR(S)				5d. PROJECT NUMBER	
				5e. TASK NUMBER	
				5f. WORK UNIT NUMBER	
7. PERFORMING ORGANIZATION NAME(S) AND ADDRESS(ES)				8. PERFORMING ORGANIZATION REPORT NUMBER	
9. SPONSORING/MONITORING AGENCY NAME(S) AND ADDRESS(ES)				10. SPONSOR/MONITOR'S ACRONYM(S)	
				11. SPONSOR/MONITOR'S REPORT NUMBER(S)	
12. DISTRIBUTION/AVAILABILITY STATEMENT					
13. SUPPLEMENTARY NOTES					
14. ABSTRACT					
15. SUBJECT TERMS					
16. SECURITY CLASSIFICATION OF:			17. LIMITATION OF ABSTRACT	18. NUMBER OF PAGES	19a. NAME OF RESPONSIBLE PERSON
a. REPORT	b. ABSTRACT	c. THIS PAGE			19b. TELEPHONE NUMBER (Include area code)

Subject terms

antibacterial; chlorhexidine diacetate; hyaluronic acid; intraosseous transcutaneous
amputation prosthesis; machining; osseointegration; polycaprolactone; surface
roughness; tensile strength; tissue adhesion; tissue engineering; titanium;
transcutaneous abutment

(The above items are included on the report cover page – Form SF298)

Table of Contents

EXECUTIVE SUMMARY	1
INTRODUCTION.....	1
METHODS, ASSUMPTIONS, AND PROCEDURES	2
DESCRIPTION OF THE COMPUTER AIDED BIOLOGY TOOL	2
BUTTON MODIFICATION.....	4
SURFACE ROUGHNESS MEASUREMENTS	4
PREPARING PCL FOR PRINTING	5
PRINTING PCL SCAFFOLDS.....	6
STRENGTH OF PCL GRIDS	7
ADHESION TESTING	7
PREPARING ANTIBACTERIAL SAMPLES.....	9
ANTIBACTERIAL ASSAY	9
ANIMAL EXPERIMENT	10
MEASUREMENT OF TENSION AT TITANIUM-SKIN INTERFACE	10
MEASUREMENT OF PRESSURE RESISTANCE AT TITANIUM-SKIN INTERFACE	10
HISTOLOGY	11
RESULTS AND DISCUSSION	11
BUTTON MODIFICATION.....	11
SURFACE ROUGHNESS	12
PRECISION OF PRINTED PCL GRIDS	12
TENSILE STRENGTH OF PCL GRIDS.....	14
ADHESION TESTING	15
ANTIBACTERIAL ASSAY	16
TENSION BUILDUP AT THE TITANIUM-SKIN INTERFACE.....	18
TISSUE ADHERENCE AT TITANIUM-SKIN INTERFACE.....	18
HISTOLOGICAL EVALUATION	19
CONCLUSION	19
PUBLICATIONS STEMMING FROM RESEARCH EFFORT	22
REFERENCES.....	22

List of Figures and Tables

FIGURE 1. COMPUTER AIDED BIOLOGY (CAB) TOOL.	3
FIGURE 2. TITANIUM BUTTON DESIGN.....	4
FIGURE 3. TITANIUM BUTTONS WITH DIFFERENT SURFACE TREATMENTS.	5
FIGURE 4. MEASURING TENSILE STRENGTH OF PCL-TITANIUM INTERFACE.	7
FIGURE 5. MODIFIED TITANIUM BUTTONS.....	11
FIGURE 6. SURFACE ROUGHNESS AND ADHESIVE STRENGTH FOR BUTTON MODIFICATIONS ..	12
FIGURE 7. PRINTED PCL GRID	13
FIGURE 8. PCL GRIDS BEFORE AND AFTER BREAKING	14
FIGURE 9. AVERAGE VIABLE BACTERIA AS SEEN BY INTERFEROMETER	16
FIGURE 10. BREAKING STRENGTH	17
FIGURE 11. WATER LEAK TEST.....	18
FIGURE 12. HISTOLOGICAL EVALUATION.....	19
TABLE 1. RMS ROUGHNESS VALUES FOR DIFFERENT SURFACE TREATMENTS.	12
TABLE 2. ANTIBACTERIAL ACTIVITY	15

Executive Summary

Introduction

Because of its high mechanical properties, chemical stability, and biocompatibility, titanium is a commonly used material in dental and orthopedic applications (Pohler 2000). Its excellent biocompatibility allows titanium implants to be directly anchored to bone, or osseointegrated (Brånemark et al., 1977; Albrektsson et al., 1981). The conventional prosthetic replacement in amputees is a stump-socket design, which transfers forces through the prosthetic to an external contact point on the patient. Such a design results in nonuniform distribution of pressure and can lead to pain, infection, and necrosis of the soft tissues at the point of contact (Dudek et al., 2006; Levy 1995).

It is believed that intraosseous transcutaneous amputation prostheses (ITAPs) can overcome these issues by directly attaching the implant to the skeleton through transcutaneous abutment (Pendegrass et al., 2008). Transcutaneous implants have been used clinically since the 1960s (Branemark et al., 1969; Branemark 1988; Branemark et al., 2001). However, subsequent attempts to use similar implants in amputees have had limited success due to problems with loosening of the implant, mechanical failure, and infection (Sullivan et al., 2003). This weak adhesion allows for invasion of bacteria at the tissue-implant interface.

It is believed that optimizing the attachment of the skin to the prosthetic will lead to clinically viable ITAPs (Pendegrass et al, 2006). Human skin is multifunctional and consequently has a complex architecture comprised of multiple layers with some

indistinct boundaries. Skin acts as an active protective agent, or barrier, against traumas such as friction, impact, pressure, and shear stress. And, many things have an effect on the properties of skin, including the location of the skin on the body, the rate of application of stress, the duration of stress, and the age of the skin (Edwards & Marks 1995).

In order to develop a clinically viable ITAP, the device must be mechanically strong, provide a tight seal at the biotic-abiotic interface, and take into account the complex properties of skin and other native tissues. Our team developed a surface modified titanium construct with an etched surface to create a surface that would allow for direct tissue adherence as well as scaffold adherence. These constructs were analyzed and adherence of a polycaprolactone (PCL) scaffold was tested both in vitro and in vivo. Our group also examined the use of different antibacterial agents to reduce bacterial invasion. It will greatly advance the application in medical field if the novel engineered titanium successfully promotes effective adhesion between the titanium-epithelium interface, thus preventing infection of the skin and underlying tissue adjacent to prosthetic implants.

Methods, Assumptions, and Procedures

Description of the Computer Aided Biology Tool

The Computer Aided Biology (CAB) Tool, which was previously known as the BioAssembly Tool or BAT (Smith et al., 2004; Smith et al., 2007), was developed to produce artificial constructs that would demonstrate properties of native tissue

(microenvironment, three-dimensional [3D] organization, and inter-cellular contact). To this end, nScript has merged techniques of digital printing and tissue engineering.



Figure 1. Computer Aided Biology (CAB) Tool. Illustration of the CAB Tool. The top panel shows a full-scale view of the tool, while the bottom panel shows a close-up view.

The CAB Tool, shown in Figure 1, utilizes a computer-aided-design/computer-aided-manufacturing (CAD/CAM) approach to build heterogeneous tissue models. This system is a multi-head, through-nozzle deposition machine developed to conformably deposit biomaterials, cells, and co-factors on various supporting surfaces to create surrogate tissues and tentative platforms for experiments in cell biology and tissue engineering. The device contains: an XY coordinate system with a stage; a number of Z-traveling deposition heads (currently up to 3), each of which is supplied with individual controlling video camera; LED work area illumination; a fiber optic light source to

illuminate the deposition area and cure photopolymers in-line; individual ferroelectric temperature controls for each deposition head; a water jacket temperature control for the stage; stainless steel and anodized work surfaces; and a piezoelectric humidifier.

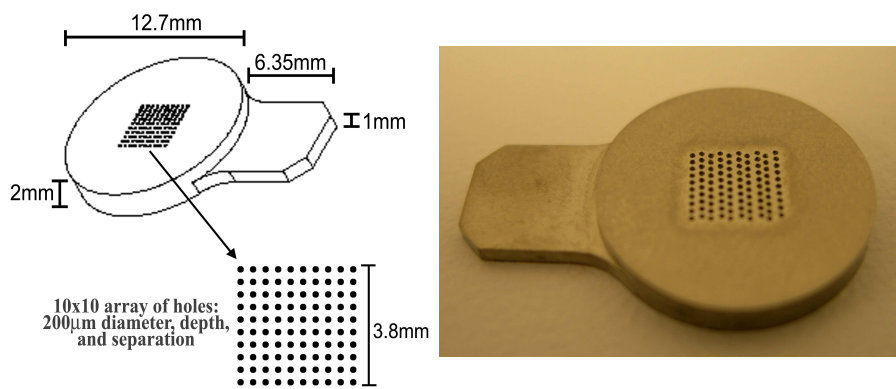


Figure 2. Titanium Button Design. A schematic drawing of the modified buttons and a representative picture of the buttons are displayed here.

Button Modification

Titanium buttons were generated from 2mm thick, known-standard titanium foil (Sigma Aldrich, St. Louis, MO). A schematic of the buttons can be seen in Figure 2. Each button was machined such that there was a 2 mm thick round section with a 12.7 mm diameter, as well as a 6.35 mm tab that is 1mm thick. All of the buttons were initially polished to a mirror finish using a coarse grit (36 grit) sandpaper followed by finer grit (400 and 800) sandpapers. The buttons were modified such that there were four groups: (1) polished buttons, (2) polished buttons with holes, (3) acid etched buttons, and (4) acid etched buttons with holes. Initially, another group of buttons was modified by sintering titanium powder on the surface of the buttons; however, this treatment group was not used in the project since the high temperature necessary for sintering oxidized the buttons. The buttons with holes (2 and 4) had a square array of 10×10 holes with 200µm diameter, depth, and separation. The total 10×10 array of holes was

3.8 mm square. The acid etched buttons (3 and 4) were etched by immersing them in a 50:40 v/v mixture of 18% HCl and 48% H₂SO₄ at 60 °C for 5 minutes. The buttons were then rinsed thoroughly in deionized water. Representative pictures of each of treatments can be seen in Figure 3.



Figure 3. Titanium Buttons with Different Surface Treatments.

Surface Roughness Measurements

The surface roughness of the acid treated and plain titanium buttons with and without holes was measured with the help of a Zygo optical interferometer running Metro Pro software. The samples were all mounted on the stage, the z-stop position was calibrated, and the light intensity was adjusted to 85-90%. The objective lens focus was adjusted until the interference fringes could be seen and the stage roll and pitch were then adjusted until the fringes covered the entire surface to be measured. Next, the software was used to capture the interference image and simultaneously reconstruct a pseudo-colored 3D profile of the surface. A region on the 3D profile was selected using the software crosshairs in order to automatically generate the average and root mean square (RMS) roughness values for that region. Three such measurements were done for the same surface and the values were averaged. The values were plotted for

the different surface treatments. A student's T test was performed to examine the significant differences between the surface treatments.

Preparing PCL for Printing

Polycaprolactone (PCL, molecular weight 80 kDa; Sigma Aldrich, St. Louis, MO) pellets were dissolved in glacial acetic acid (Sigma Aldrich, St. Louis, MO) at a concentration of 70% w/v. This concentration was found to be best for dispensing and ease of solvent evaporation, resulting in a solid structure. The mixture of PCL pellets and acetic acid was placed in a glass bottle with a sealed cap, and the solution was dissolved using a sonicator for 1-2 hours. After the PCL was fully dissolved, the solution was stirred with a spatula, backfilled into a 3-mL dispensing syringe (EFD, Providence, RI), closed with a stopper at the bottom and top of the syringe, and spun in a centrifuge at 2000 rpm for 5 minutes to remove air bubbles. This solution was then used for scaffold printing.

Printing PCL Scaffolds

The syringe was connected to an air pressure line for dispensing of the PCL solution. The ceramic dispensing tip used had an inner diameter of 100 μm and outer diameter of 150 μm . A pressure of 25 psi was used to push the PCL solution through the ceramic tip orifice and deposit onto the target substrate. The printing speed (both XY stage and Z movement) of the dispensing pump was 2.5 mm/s. The speed is very important to the rate of evaporation of the acetic acid solvent, which therefore affected the creation of pores within the scaffold. A script (pen path) was created in AutoCAD and used to print the PCL scaffolds. The initial dispensing height was 50 μm and a lift of

25 μm between each layer. Scaffold designs were entered into the PathCAD program to generate porous constructs that were 5.4 mm \times 5.4 mm. A single line of extrusion was used to generate the struts; thus, the designed strut thickness (width of the lines used to fabricate the PCL scaffold) was 100 μm . The input pore size (the open space in between the lines of PCL) was 300 μm . This scaffold was designed to be 130 μm tall, with a strut thickness of 100 μm . The printed scaffolds were measured, and the measured values were compared with the expected values.

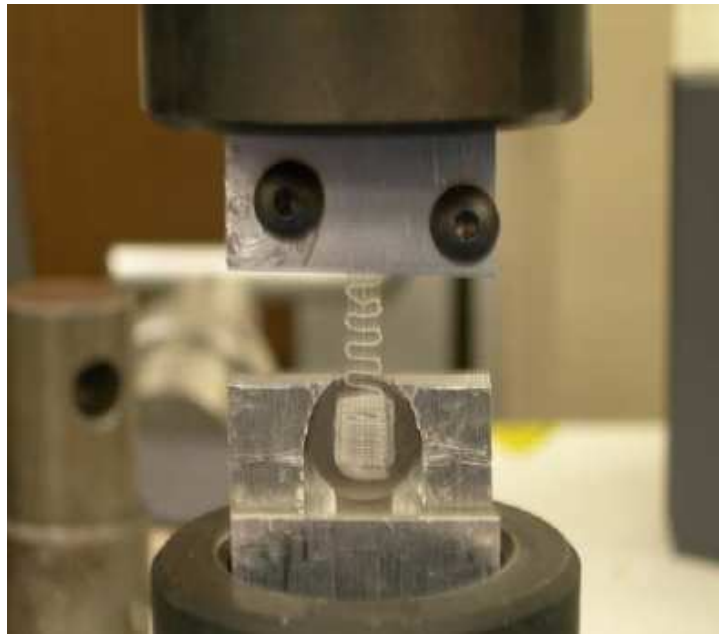


Figure 4. Measuring Tensile Strength of PCL-Titanium Interface.

Strength of PCL Grids

Preliminary mechanical testing was conducted with a specially designed scaffold (Figure 8a). This scaffold was designed to be similar to the scaffolds printed on the titanium buttons, with a height of 130 μm and a strut thickness of 100 μm . The scaffolds were longer (10 mm) and were wider at one end. To test the strength of the scaffold, the narrower end was fixed and the wider end was pulled until the scaffold broke. The force

required to break the scaffolds was recorded, and the ultimate strength was calculated by dividing the force with the effective cross-sectional area (0.169 mm^2).

Adhesion Testing

A tensiometer (Instron 3369, Instron Corp., Norwood, MA) was used to examine the peel off adhesion test for the PCL. A modified PCL grid was printed on the buttons for adhesion testing. These grids were printed such that there was a section of the grid hanging over the edge of the button (See Figure 8c). As can be seen in Figure 4, an aluminum jig was manufactured (in house) in order to attach the tensiometer to the PCL on the button. This jig had one plate with a circular groove in it where the buttons were placed and another aluminum plate was placed over it and screwed into place to secure the button. This section was attached to one end of the tensile tester. The free end of the printed PCL was glued to another plate, which was attached to the other testing end of the tensile tester. The crossheads were moved in opposite directions producing a tensile force on the PCL-titanium interface. The crosshead speed was set at 3 mm/min. The test was carried out till either the PCL peeled off from the titanium substrate or broke into two pieces. The software also generated values for the break load, maximum load, and the maximum displacement. The stress (MPa) vs. strain curves were calculated, and the adhesion strength (MPa) for each surface treatment was assigned the value of the maximum stress from the corresponding curve. Three measurements were done for each surface treatment and the values were then averaged and the standard deviations were calculated and plotted. A student's T test was performed to examine the significant differences between the surface treatments.

Preparing Antibacterial Samples

Type I collagen (Col) and hyaluronic acid (HA) solutions were mixed with one of three antibacterial materials, either silver nanoparticles (Ag; Sigma Aldrich, St. Louis, MO), Titanium dioxide anatase (TiO₂; Sigma Aldrich, St. Louis, MO), or chlorhexadine diacetate (ChD; Sigma Aldrich, St. Louis, MO). A 3.0 mg/mL collagen solution was prepared as previously described (Smith 2004). Briefly, purified rat-tail collagen type I (BD Biosciences, Bedford, MA) was mixed with 4× Dulbecco's Modified Eagle's Medium (DMEM) and brought to a pH of 7.0-7.4 by the addition of 1 M NaOH. A solution of HA was prepared from an Extracel™ Hydrogel kit (Glycosan Biosystems, Inc., Salt Lake City, UT) by following the given protocol. After the Col or HA solution was prepared, an antibacterial agent was mixed into the solution at 1-10% w/w by gently pipetting. Next, 100 µL of the solution was placed in a 6 well plate and allowed to fully polymerize at 37 °C for 1 hour.

Antibacterial Assay

Staphylococcus aureus (ATCC, Manassas, VA) was grown in Caso broth (casein-peptone soymeal-peptone broth) overnight at 37°C in a water bath. The antibacterial samples (described above) were incubated at 37°C for 1 hour in the Caso broth solution containing *S. aureus*. Aliquots of broth were obtained from each group. The aliquots were stained with Crystal Violet for 15 minutes, and an acetic acid solution was added to solubilize the stained bacteria in the broth. The bacteria were then quantified using a spectrofluorometer at 630 nm.

Animal Experiment

Before transplantation of the titanium button subcutaneously, the rats were administered inhaled anesthesia using isoflurane. Pre-emptive analgesia was given 30 minutes before the procedure as a subcutaneous injection of buprenorphine on a clean pathogen free surgical table. Following surgical area preparation, two 2 cm dorsal incisions were carried down to the fascia. Using blunt dissection, autoclaved titanium discs were tunneled subcutaneously. The discs were maintained subcutaneously for a period of time and the tension between cutaneous tissue and titanium interface was measured.

Measurement of Tension at Titanium-Skin Interface

A tensiometer (Instron 4442, Instron Corp., Norwood, Massachusetts) was used to test breaking strength. Briefly, the skin and underlying disc was removed en-block measuring appropriately 4 cm × 4 cm from the animal back. To determine the break strength, the skin part was attached to one grip of the equipment while the titanium disc was tied to the opposite grip. The break strength at the skin-titanium interface was measured dynamically.

Measurement of Pressure Resistance at Titanium-Skin Interface

A cylinder was mounted around the titanium-skin interface. The cylinder was kept vertical. The lumen of the cylinder was loading with water to gradually increase the water pressure on the titanium-skin interface until the water was observed. The height of the water required to disrupt the interface reflected the pressure resistance at the

titanium-skin interface. This method was used on the rationale that with prostheses, any break in the adhesion would lead to late failure in the implant, and so this technique allowed measurement of the weakest point of adherence.

Histology

Following transplantation of the titanium discs for a period of time, the skin and the underlying titanium were carefully separated and the cutaneous tissue was fixed in 10% formalin, paraffin-embedded and hematoxylin-eosin-stained.

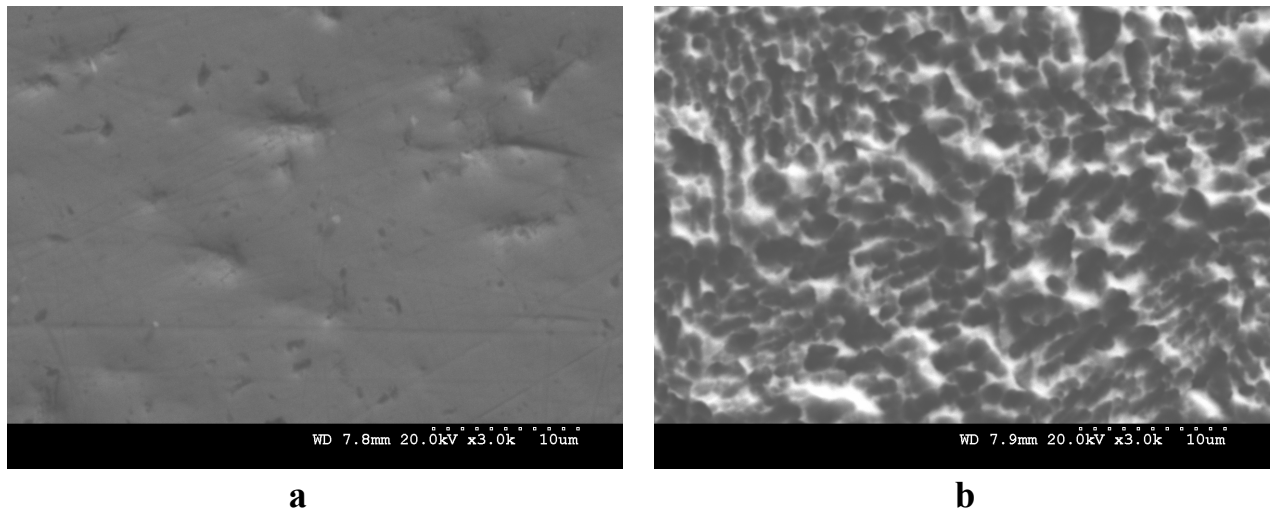


Figure 5. Modified Titanium Buttons. SEM images were taken of the surfaces of the buttons that were both (a) polished and (b) acid etched.

Results and Discussion

Button Modification

As can be seen in Figure 2, buttons were machined from 2 mm thick titanium foil such that there was a 2 mm thick round section with a 12.7 mm diameter and a 6.35 mm long tab that was 1 mm thick. Half of the buttons had a 10×10 array of holes that

were 200 μm in diameter, depth, and separation. All of the buttons were polished to a mirror finish. Then, half of the holed buttons and half of the non-holed buttons were acid etched to increase surface roughness.

RMS Roughness (μm)	P	H	AE	AEH
Average	0.338	0.344	1.232	1.388
Standard Deviation	0.065	0.075	0.250	0.222

Table 1. RMS Roughness Values for Different Surface Treatments.

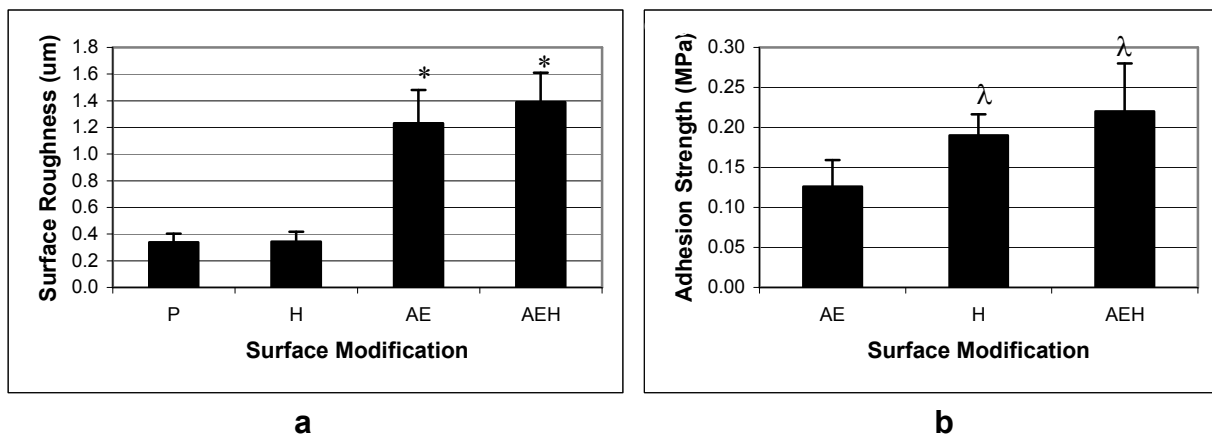


Figure 6. Surface Roughness and Adhesive Strength for Button Modifications. (a) The root mean square surface roughness was measured with an interferometer to determine the difference in the surfaces of polished buttons (P), polished buttons with holes (H), acid etched buttons (AE), and acid etched buttons with holes (AEH). (b) The adhesive strength was tested for the groups: AE, H, and AEH. * Indicates a significant increase in the surface roughness of the buttons as compared with polished buttons ($p < 0.05$). λ Indicates a significant increase in strength as compared with acid etched buttons ($p < 0.08$).

Surface Roughness

Using a Zygo optical interferometer, the RMS surface roughness was measured for the groups of buttons: polished without holes (P), polished with holes (H), aid etched without holes (AE), and acid etched with holes (AEH). These results can be seen in Table 1 as well as in the graph in Figure 6a. There was no significant difference in the

surface roughness of the two polished groups (P and H). There was a significant increase in the surface roughness of the acid etched groups (AE and AEH) when compared to the polished buttons.

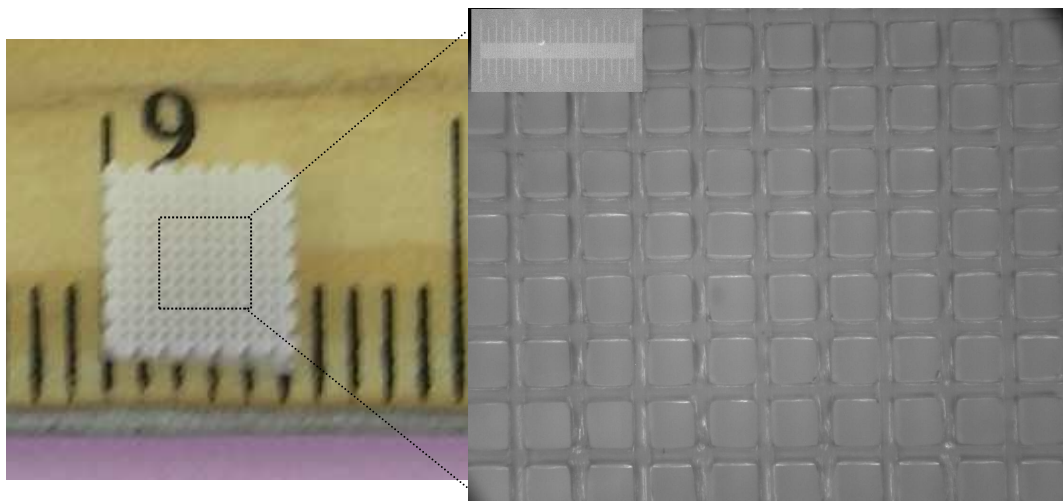


Figure 7. Printed PCL Grid. A representative picture of a printed PCL grid can be seen. This shows the whole grid as well as a high-resolution picture showing the uniformity of the struts and pores of the grid (unit in mm).

Precision of Printed PCL Grids

Porous scaffolds are sometimes desired to provide an area for cells to migrate and proliferate or for controlled release of chemicals (Leong et al., 2001). The CAB tool can print complex 3D scaffolds with different designs in terms of overall shape, dimension, and pore size. In order to test the accuracy of the CAB tool using 70% PCL, a 5.4 mm × 5.4 mm × 1.5 mm (L×W×H) scaffold was fabricated. Figure 7 demonstrates a representative scaffold that was printed using the CAB tool. It is clear from looking at this figure that the struts and pores within the scaffold are uniform and evenly spaced. The printed scaffolds were measured and the measured values were compared with the expected values. A single, non-overlapping line was extruded in order to generate each

strut within the scaffolds. Since the dispensing tip used had an inner diameter of 100 μm , the expected strut size was 100 μm . The pore size (the open space in between the lines of PCL) that was programmed into the script was 300 μm . The measured strut size was $65 \pm 12 \mu\text{m}$; and the measured pore size was $315 \pm 10 \mu\text{m}$. The overall porosity of the scaffolds was $54 \pm 1\%$.

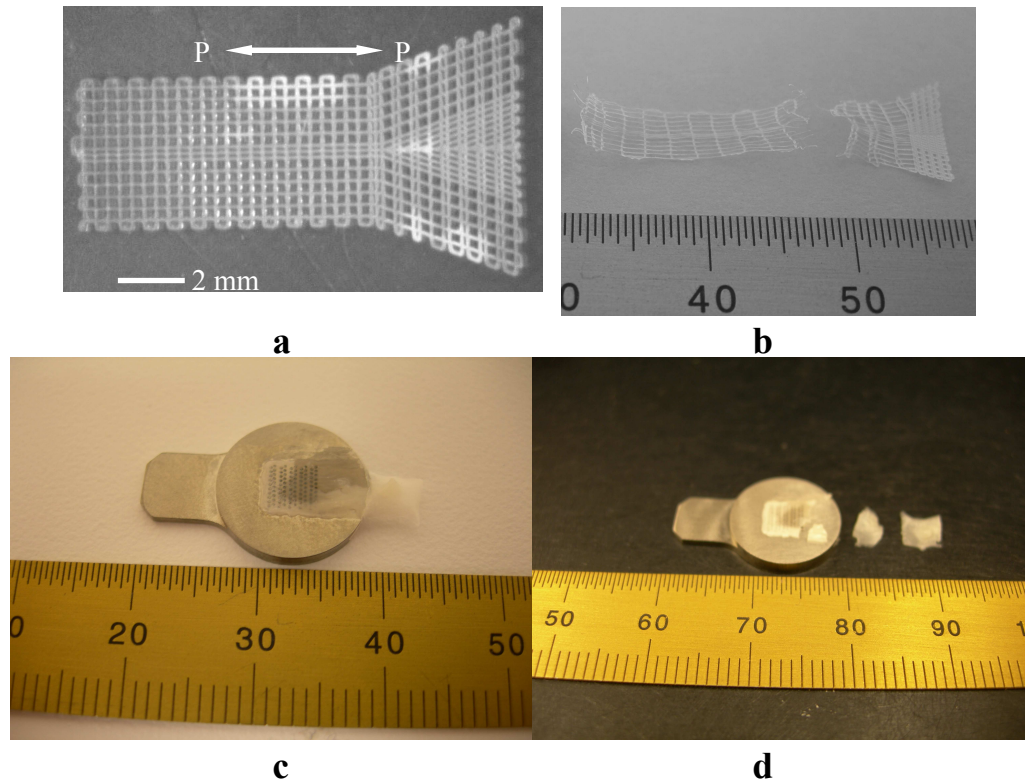


Figure 8. PCL Grids Before and After Breaking. PCL grids were tested for strength both on and off of the titanium buttons. (a) Specially designed PCL grids were printed and (b) stretched until they broke apart. (c) PCL grids were also printed on the titanium buttons and (d) stretched until they either broke or came off of the buttons.

Tensile Strength of PCL Grids

To demonstrate that the printing process of the CAB tool does not significantly alter the strength of the printed PCL, a special scaffold design was entered into the PathCAD software. A sample of this scaffold can be seen in Figure 8. These scaffolds

were able to hold between 4-8 pounds before ultimately breaking. Using the effective cross sectional area of 0.169 mm^2 , the ultimate strength varied from 24 to 40 MPa with an average of 29.62 MPa.

Treatment	Percent
None	100.00
Col Alone	94.73
Col + 10 % w/w Ag	117.97
Col + 10% w/w ChD	80.62
<i>Col + 10 % w/w TiO₂</i>	<i>27.38</i>
HA Alone	106.56
HA + 10% w/w Ag	104.90
<i>HA + 10% w/w ChD</i>	<i>15.23</i>
<i>HA + 10 % w/w TiO₂</i>	<i>17.80</i>

Table 2. Antibacterial Activity. The antibacterial activity of 10% w/w solutions of Ag, ChD, and TiO₂ in either Col or HA were compared. These values were compared to the bacteria in broth. A percent value was calculated as the percentage of bacteria seen in the treatment group compared with the bacteria in broth and no treatment. A significant decrease was only seen in the italicized groups.

Adhesion Testing

When PCL was printed on top of smooth Titanium buttons, the PCL peeled off of the buttons upon drying. When the Titanium buttons were either acid etched or holes were added to the button surface, the PCL would remain on the Titanium button. The different surface modifications were examined to determine which provided the best adhesion between the PCL and the button. The average adhesive strengths for the acid etched buttons (AE), polished buttons with holes (H), and acid etched buttons with holes (AEH) can be seen in Figure 6b. Buttons that were acid etched, had an average adhesive strength of 0.13 MPa. When holes were added to the buttons, there was a

significant increase in the adhesive strength as compared with acid etched buttons with no holes. And, while there was a slight increase in the average adhesive strength, we did not see a significant difference between holed buttons that were acid etched as compared with holed buttons that were polished. Thus, the addition of holes gave the desired result of a significant increase in adhesive strength.

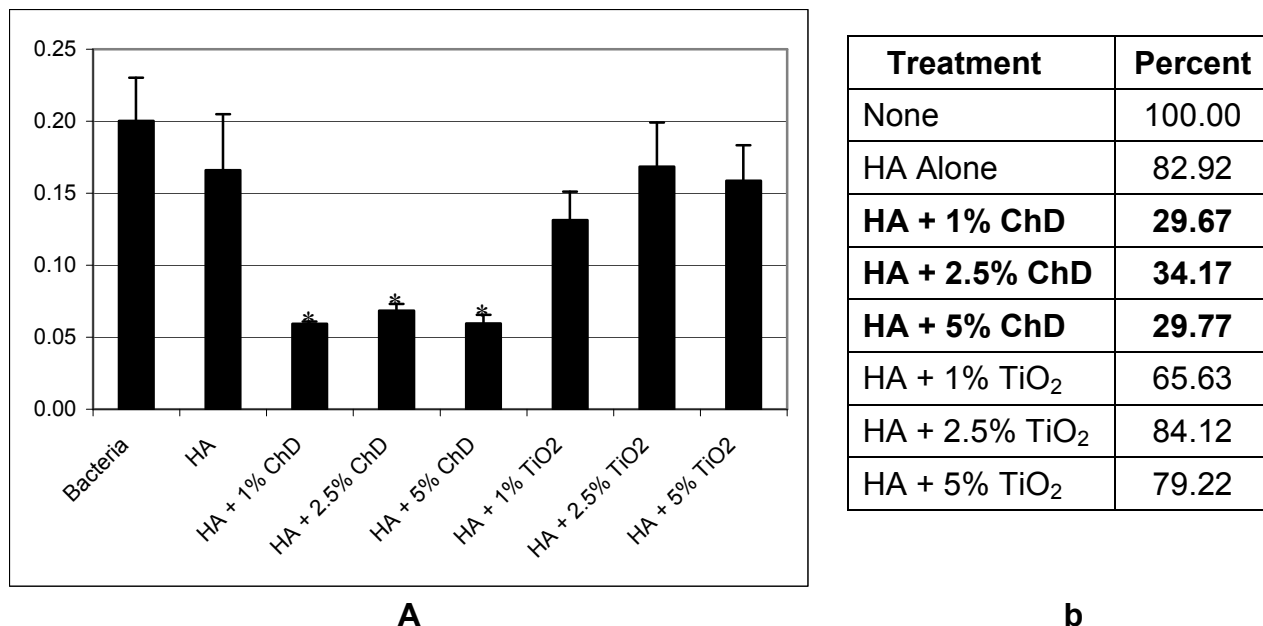


Figure 9. Average Viable Bacteria as Seen by Interferometer. (a) Viable bacteria seen with various antibacterial agents mixed in the Hyaluronic Acid (HA): 1% w/w ChD, 2.5% ChD, 5% ChD, 1% w/w TiO₂, 2.5% TiO₂, and 5% TiO₂. * Indicates a significant decrease in bacterial viability when compared with HA alone. (b) The percentage of bacteria seen in treatment groups using bacteria in broth as the standard number of bacteria in broth at the same time point. A significant decrease from the non-treatment group was only seen in the bold groups.

Antibacterial Assay

Initially, we examined using different antibacterial agents (Silver nanoparticles [Ag] and Titanium Dioxide Anatase [TiO₂]) within the PCL or coating the PCL. However, we were not able to see a significant decrease in the viable bacteria when using these

methods. Based on these results, we decided to examine the antibacterial activity of different antibacterial agents (of Ag, TiO_2 , and Chlorhexidine Diacetate [ChD]) embedded in natural biomaterials type I Collagen (Col) or Hyaluronic Acid (HA). There was no significant difference in the viable bacteria seen on either Col alone or HA alone when compared with the bacteria broth. Table 2 demonstrates the percentage of bacteria seen in treatment groups using bacteria in broth as the standard number of bacteria in broth at the same time point. A significant decrease in bacteria was seen when 10% w/w TiO_2 was added to either Col or HA. Also, a significant decrease in bacteria was seen when 10% w/w ChD was added to HA. This decrease was not significant when the ChD was added to Col. Because we saw a significant decrease in bacteria in the treatment groups using HA with varying concentrations of either ChD or TiO_2 (1% - 5% w/w). Figure 9 shows the interferometer results. There was no significant decrease in the bacteria when TiO_2 was used. However, there was a significant decrease in bacteria when any concentration of ChD was added to the HA.

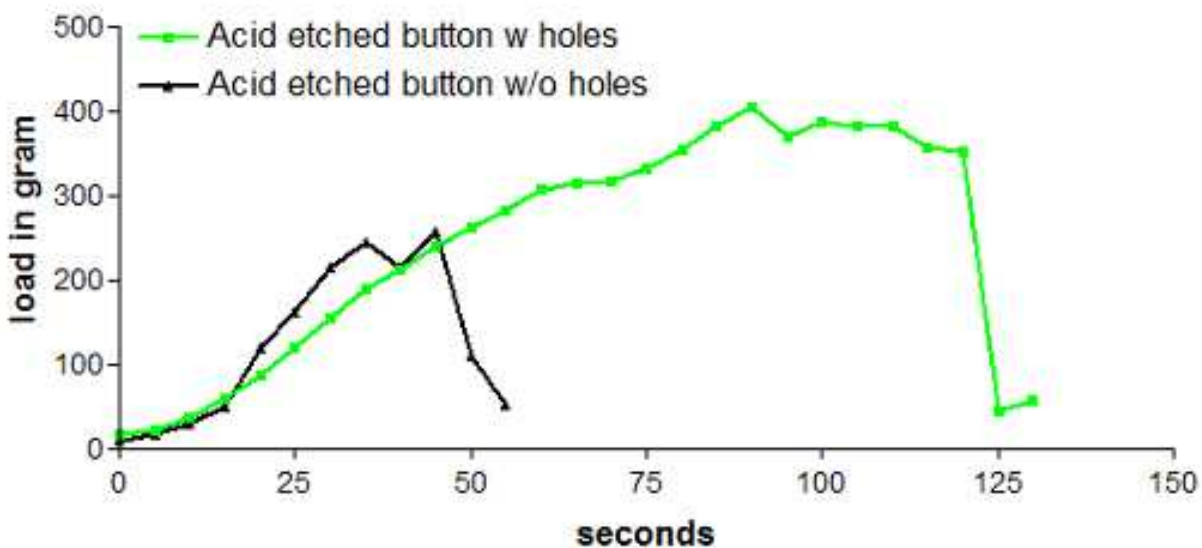


Figure 10. Breaking Strength. Breaking strength seen between the titanium disc and adjacent tissue following implantation for 43 days.

Tension Buildup at the Titanium-Skin Interface

Using an Instron 4442 tensiometer as described in the methods section, the tension at the titanium-skin interface was measured following implantation of titanium discs for 43 days. As shown in Figure 10, the tension at the interface is higher with acid etched button with holes than acid etched buttons without holes. This experiment was encouraging, suggesting that the surface etched buttons had improved adherence in soft tissue, and provided a rationale for continued experiments.

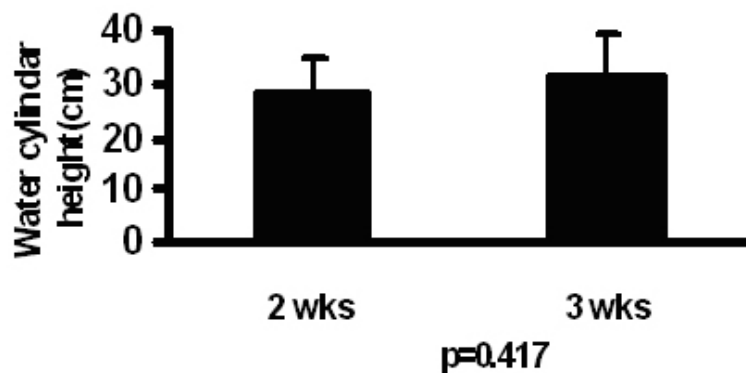


Figure 11. Water Leak Test. Tissue adherence as measured by water pressure tolerance at the titanium-skin interface.

Tissue Adherence at Titanium-Skin Interface

Tissue adherence as measured by water pressure tolerance at the titanium-skin interface. This experiment was done to determine whether interaction between skin and titanium was enhanced with prolonged implantation of the surfaced materials. As shown in Figure 11, pressure resistance gradually increased with prolonged implantation of the titanium materials, although this did not reach statistical significance. In these set of experiments, the button was implanted subcutaneously and then the skin incised after three weeks, and the button brought through the skin to allow

measurement of adherence (as measured by water leakage or water pressure) over time.



Figure 12. Histological Evaluation. Three weeks after the titanium button was implanted subcutaneously, a 3mm punch was made to expose the nipple. Two weeks following, the tissue was harvested and prepared for histology. The center space of the picture was originally occupied by the nipple of the button. The epidermis of wound edge crawled down along the nipple.

Histological Evaluation

As shown in Figure 12, first, the inflammation was moderate and not intense in the tissue surrounding titanium discs suggesting that the modified materials are well compatible with living tissue. Second, a fibrous tissue cyst surrounding the implanted titanium disc is formed indicating the living tissue has a potential to grow into to pores within the titanium, therefore, possible barrier to prevent invasion of microorganisms to the deep tissue.

Conclusion

When using the CAB Tool to generated spatially organized 3D PCL constructs, we concluded that a 70% solution of PCL in acetic acid was the best concentration to use for consistency in printing. When a 100 μm ceramic tip was used to extrude the PCL, the average width of the printed lines was $65 \pm 12 \mu\text{m}$. And, with a programmed pore size of 300 μm , the measured pore size was $315 \pm 10 \mu\text{m}$. These constructs were

then examined for their tensile strength and the average ultimate strength was between 29-42 MPa. The tensile strength of human skin has been measured as 17 – 21 MPa (Edwards & Marks 1995).

When PCL was printed on top of smooth Titanium buttons, the PCL peeled off of the buttons upon drying. When Titanium buttons were either acid etched or the surface was machined with an array of holes, the PCL was able to adhere to the Titanium. Buttons that were acid etched, had an average adhesive strength of 0.13 MPa. A significant increase in the adhesive strength was witnessed when an array of holes was added to the surface of the Titanium. The adhesive strength increased to 0.19 MPa for buttons with only holes (H) and to 0.22 MPa for buttons with both holes and acid etching (AEH). Thus, the addition of the array of holes does significantly increase the adhesive ability of Titanium. Orr et al. (1999), defined an adhesive as a material that exhibited an adhesive strength of greater than 0.1 MPa, and materials that had an adhesive strength lower than this were sealants. With an adhesive strength of 0.22 MPa, printing a PCL grid on an acid etched and machined (AEH) titanium is an adhesive, and can be effectively treated as a bio-concrete.

When an antibacterial agent was added to the PCL or placed on the titanium button, we did not see a significant decrease in the number of viable bacteria when compared with bacteria in culture. However, when an antibacterial agent was added to type I collagen or hyaluronic acid, we did see a decrease. To minimize the chance of developing a resistant strain of bacteria, we examined using a smaller concentration of antibacterial agent within the collagen or HA. It was noted that 1% (w/w) chlorhexidine diacetate in HA was as effective as a 5% (w/w) concentration. It was noted that the

percent of viable bacteria was lower in a 10% solution. Thus, more research should be conducted to determine the best concentration to use to prevent bacterial invasion while also promoting cell viability.

When these constructs were tested in vivo, we saw that the tension at the interface is higher with acid etch buttons with holes as compared with acid etched buttons without holes. We also noticed a slight, although not significant, increase in pressure resistance at the surface of the implanted constructs when they were implanted for 3 weeks as opposed to 2 weeks. No significant inflammation was seen around the implanted constructs, and a fibrous tissue cyst formed surrounding the implanted titanium disc. These in vivo results indicate that our specially machined buttons have the potential for growth of cells within the pores of the titanium disc as well as increased adherence of soft tissue.

These experiments made some important observations. First, and foremost, our study design and animal model demonstrated the feasibility of these experiments in testing prototypes for optimizing the epithelial prosthesis interface. We had to employ several novel design elements, and our design was successful. Secondly, our study showed that the modified titanium material has an advantage over the plain titanium material to maintain a better interface interaction. However, more experiments are needed to draw a conclusion.

Future experiments need need to be planned to further varify the antibacterial properties of chlorhexidine diacetate in hyaluronic acid. An experient examining the release of the chlorhexidine diacetate would be beneficial. Similarly, it will be interesting to determine whether the antibacterial materials applied to the etched surface could

retard bacterial proliferation and biofilm, and matrix molecules could further promote cellular adherence in vivo.

We believe that based on the experimental results we have demonstrated, that by machining the surface of the titanium, the 70% PCL adheres to the surface like a bioconcrete. By adding a natural biopolymer such as HA or collagen and mixing it with an antibacterial agent, the Titanium will not only exhibit adhesion but also prevent bacterial invasion. Thus, such a construct is an excellent candidate for studies in generating ITAPs.

Publications Stemming from Research Effort

Cynthia M. Smith, Ken Church, Bo Li, Tithi Dutta-Roy, Abhijeet Bhalkikar, James Hickman. Development of a novel titanium surface that promotes adhesion. *Working Paper 2008*.

References

Albrektsson T, Bränemark PI, Hansson HA, and Lindström J. Osseointegrated titanium implants: Requirements for ensuring along-lasting, direct bone-to-implant anchorage in man. *Acta Orthop Scand* 1981;52:155–170.

Bränemark PI, Breine U, Adell R, and Breine U. Intra-osseous anchorage of dental prostheses. *Scand J Plast Recon Surg* 1969;3:81-100.

Bränemark PI, Hansson BO, Adell R, Breine U, Lindström J, Hallen O, and Ohman A. Osseointegrated implants in the treatment of the edentulous jaw: Experience from a 10-

year period. Scand J Plast Reconstr Surg Suppl 1977;16:1–132.

Bränemark PI. Tooth replacement by oral endoprostheses: clinical aspects. Int J Oral Implantol 1988;5:27-9.

Bränemark R, Branemark PI, Rydevik B, and Myers RR. Osseointegration in skeletal reconstruction and rehabilitation: a review. J Rehabil Res Dev 2001;38:175-81.

Dudek NL, Marks MB, and Marshall SC. Skin problems in an amputee clinic. Am J Phys Med Rehabil 2006;85:424-9.

Edwards C and Marks R. Evaluation of biomechanical properties of human skin. Clin Dermatol. 1995 Jul-Aug;13(4):375-80.

Leong KF, Phua KK, Chua CK, Du ZH, and Teo KO, Fabrication of porous polymeric matrix drug delivery devices using the selective laser sintering technique. Proc Inst Mech Eng H 2001; 215:191–201.

Levy SW. Amputees: skin problems and prostheses. Curtis 1995;55:297-301.

Orr TE, Patel AM, Wong B, Hatzigiannis GP, Minas T, and Spector M. Attachment of periosteal grafts to articular cartilage with fibrin sealant. J Biomed Mater Res. 1999; 44(3):308-13.

Pendegrass CJ, Goodship AE, Price JS, and Blunn GW. Nature's answer to breaching the skin barrier: an innovative development for amputees. J Anatomy 2006;209:59-67.

Pendegrass CJ, Gordon D, Middleton CA, Sun SN, and Blunn GW. Sealing the skin barrier around transcutaneous implants: in vitro study of keratinocyte proliferation and

adhesion in response to surface modifications of titanium alloy. J Bone Joint Surg Br. 2008;90(1):114-21.

Pohler OE. Unalloyed titanium for implants in bone surgery. Injury. 2000;31 Suppl 4:7-13.

Smith CM, Stone AL, Parkhill RL, Stewart RL, Simpkins MW, Kachurin AM, Warren WL, and Williams SK. Three-dimensional bioassembly tool for generating viable tissue-engineered constructs. Tissue Eng. 2004;10(9-10):1566-76.

Smith CM, Christian JJ, Warren WL, and Williams SK. Characterizing environmental factors that impact the viability of tissue-engineered constructs fabricated by a direct-write bioassembly tool. Tissue Eng. 2007;13(2):373-83.

Sullivan J, Uden M, Robinson KP, and Sooriakumaran S. Rehabilitation of the trans-femoral amputee with an osseointegrated prosthesis: the United Kingdom experience. Prosthet Orthot Int 2003;27:114-20.